Higgs Boson **Mass** and Width

Waltteri Leinonen

On behalf of the ATLAS Collaboration

July 10th, 2025

ATLAS EXPERIMENT
Nikhef
Radboud University

Outline

m_H

- Free parameter in the SM
- Determines all other properties e.g. CP, branching ratios, $\boldsymbol{\Gamma_H}$

Precision Higgs mass measurement in $H \to ZZ$ and $H \to \gamma\gamma$

- $H \to \gamma\gamma$: Phys. Lett. B 847 (2023) 138315
- $H \to ZZ^* \to 4l$: Phys. Lett. B 843 (2023) 137880
- Combination : Phys. Rev. Lett. 131 (2023) 251802

Γ_H

- <u>Total</u> Higgs decay width, calculated **~4.07 MeV** in the SM at measured Higgs mass
- **Sensitive to BSM**

Constraining Higgs width from off-shell $H \to VV$ and $H \to t\bar{t}$

- $H^* \to ZZ \to 4l$: Rep. Prog. Phys. 88 057803 (2025)
- $H* \to WW \to l\nu l\nu$: CERN-EP-2025-059
- $\mathrm{pp} \to t\bar{t}t\bar{t}$: Phys. Lett. B 861 (2025) 139277

$$p_{Tt}^{\gamma\gamma} = |\vec{p}_T^{\gamma\gamma} \times \mathit{thrust}_{\gamma\gamma}|$$

Mass: $H \rightarrow \gamma\gamma$

Events must have ≥ 2 photon candidates (tight ID, loose isolation).

- $105\ \text{GeV} < m_{\gamma\gamma} < 160\ \text{GeV}$
- $\left(p_T^{\gamma_1} > 0.35 \times m_{\gamma\gamma}\right) \cap \left(p_T^{\gamma_2} > 0.25 \times m_{\gamma\gamma}\right)$

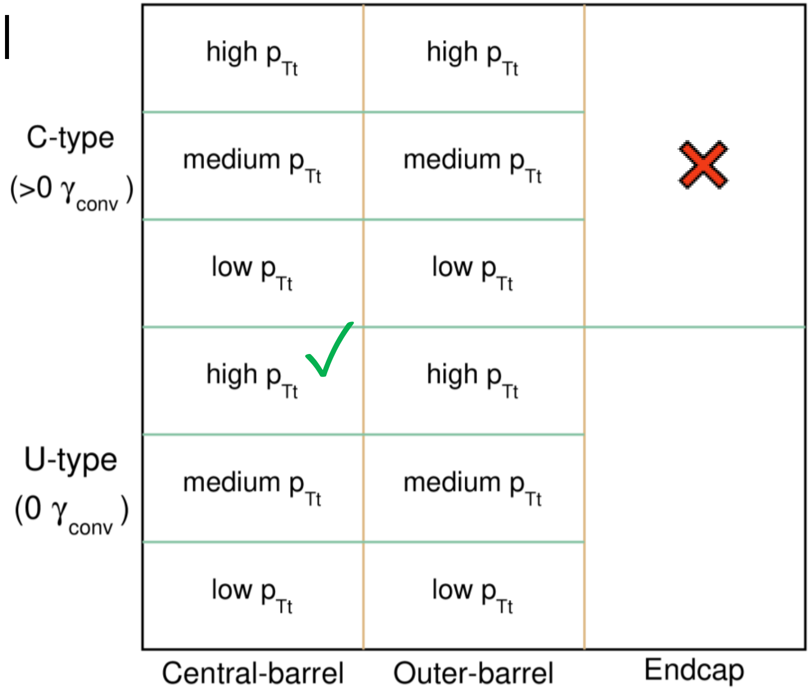

Events split into 14 categories with higher/lower:

- **Energy scale uncertainties**
- **$m_{\gamma\gamma}$ resolution**
- **Signal–to–background ratio**

17% resolution improvement from splitting alone

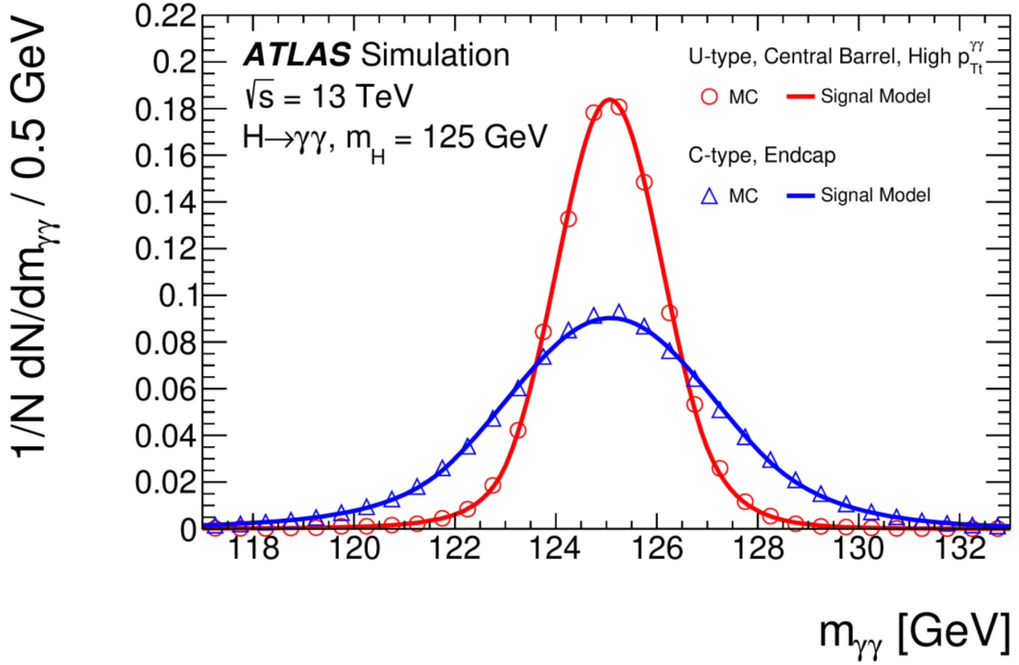

Mass: $H \to \gamma\gamma$

Significant improvements from **new photon reconstruction algorithm** and **photon energy calibration** using $Z \to e^+e^-$

Photon energy calibration : 320 MeV → 83 MeV

- Biggest impact $Z \to e^+e^-$ electron energy **linearity fit**
- Constrain E_T-dependent electron energy scale

Background interference (1-2% shift): ± 26 MeV

Source	Impact [MeV]
Photon energy scale	83
$Z \to e^+e^-$ calibration	59
E_{T}-dependent electron energy scale	44
$e^\pm \to \gamma$ extrapolation	30
Conversion modelling	24
Signal–background interference	26
Resolution	15
Background model	14
Selection of the diphoton production vertex	5
Signal model	1
Total	90

Overall x4 reduction of systematics

330 MeV → 90 MeV

Mass: $H \to \gamma\gamma$

Signal modeled in MC with double-sided crystal ball func.

Non-resonant $\gamma\gamma$-background modelled by template fit to $m_{\gamma\gamma}$ sidebands. Systematics derived from templates of background MC in 3 “loose-not-tight” regions.

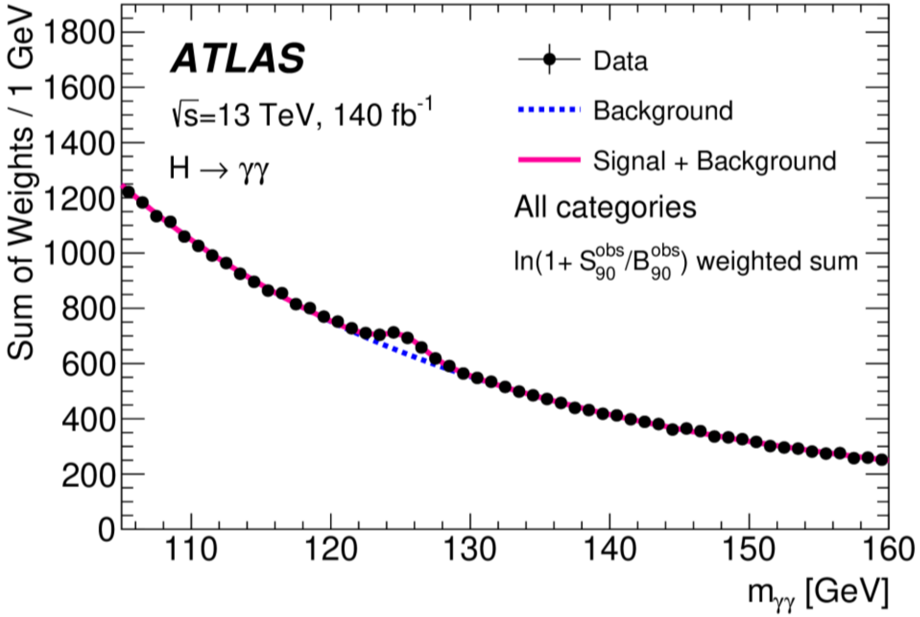

‰ -level precision in the Run-1+Run-2 combination

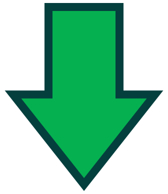

Highest precision on m_H in a single Higgs decay channel!

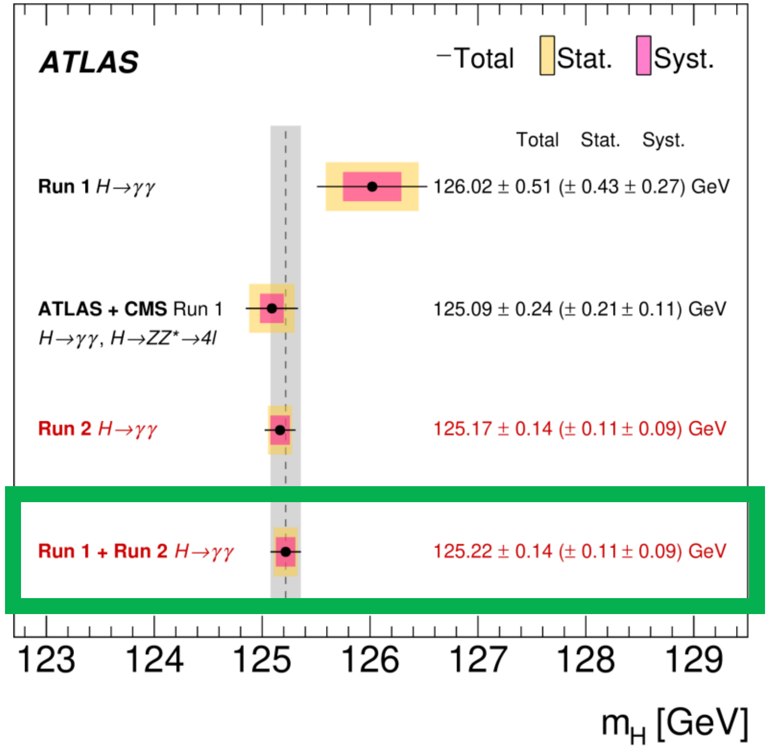

Mass: $H \rightarrow ZZ \rightarrow 4l$

High purity lepton quadruplet sub-channels
$(4\mu, 2e2\mu, 2\mu2e, 4e)$ **low stat. compared to $H \rightarrow \gamma\gamma$**

Systematics reduced multiple ways:

- Lepton momentum calibrated from $J/\Psi \rightarrow \mu^+\mu^-$, and $Z \rightarrow l^+l^-$ events

  x4 reduction in associated uncertainties

- **Kinematic refit** of leading dilepton in m_Z

  17% better m_{4l} mass resolution

- **m_{4l} mass resolution enhanced by quantile regression neural net (QRNN)**

  Reduces total m_H uncertainty by 1% when included in the likelihood

Event-level resolution (QRNN)

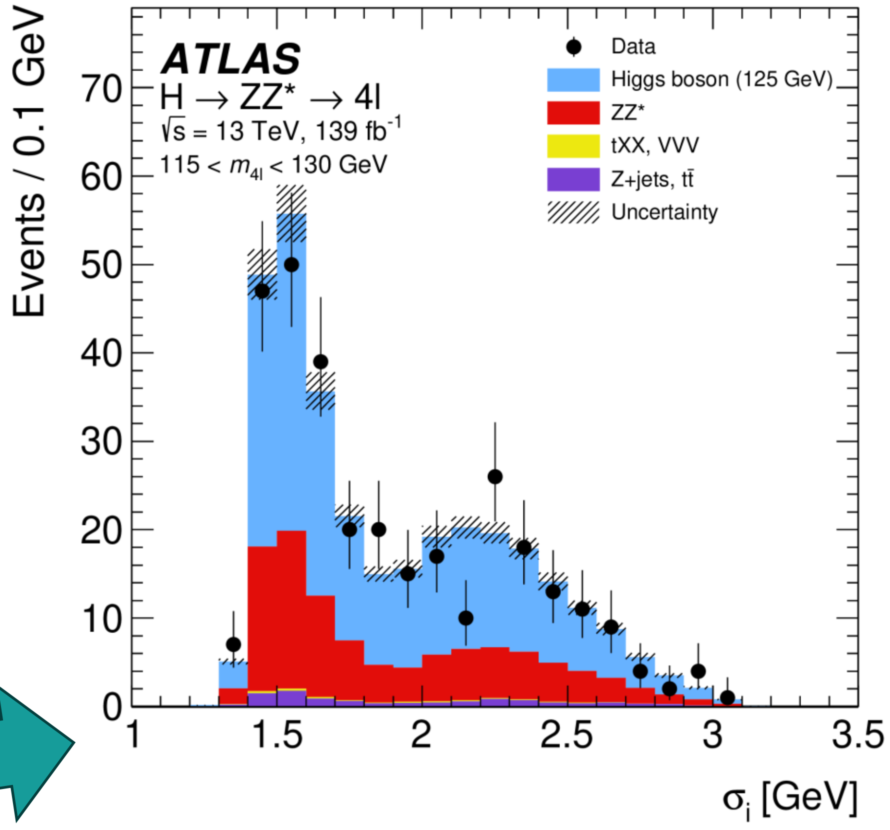

Mass: $H \to ZZ \to 4l$

A classification DNN trained in each sub-channel purifies signal from non-resonant ZZ backgrounds.

Unbinned profile LH fit is performed across sub-channels - **improves sensitivity and resolution**

Systematic Uncertainty	Contribution [MeV]
Muon momentum scale	± 28
Electron energy scale	± 19
Signal-process theory	± 14

Final state	Higgs	ZZ, tXX, VVV	Reducible backgrounds	Expected total yield	Observed yield	S/B
4μ	78 ± 5	38.7 ± 2.2	2.84 ± 0.17	120 ± 5	115	1.89
$2e2\mu$	53.4 ± 3.2	26.7 ± 1.4	3.02 ± 0.19	83.1 ± 3.5	94	1.80
$2\mu 2e$	41.2 ± 3.0	17.9 ± 1.3	3.4 ± 0.5	62.5 ± 3.3	59	1.93
$4e$	36.2 ± 2.7	15.7 ± 1.6	2.83 ± 0.35	54.8 ± 3.2	45	1.95
Total	209 ± 13	99 ± 6	12.2 ± 0.9	321 ± 14	313	1.88

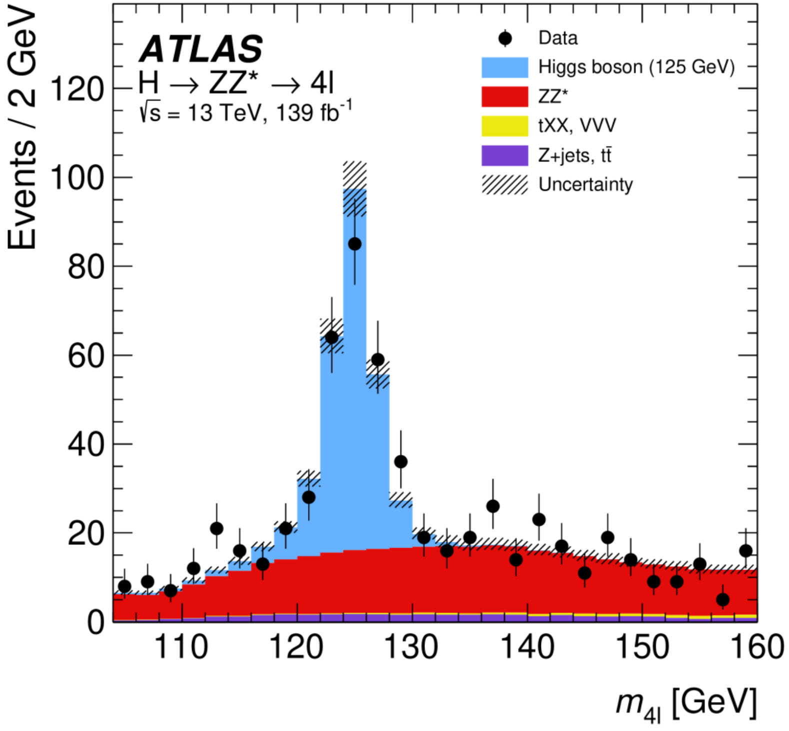

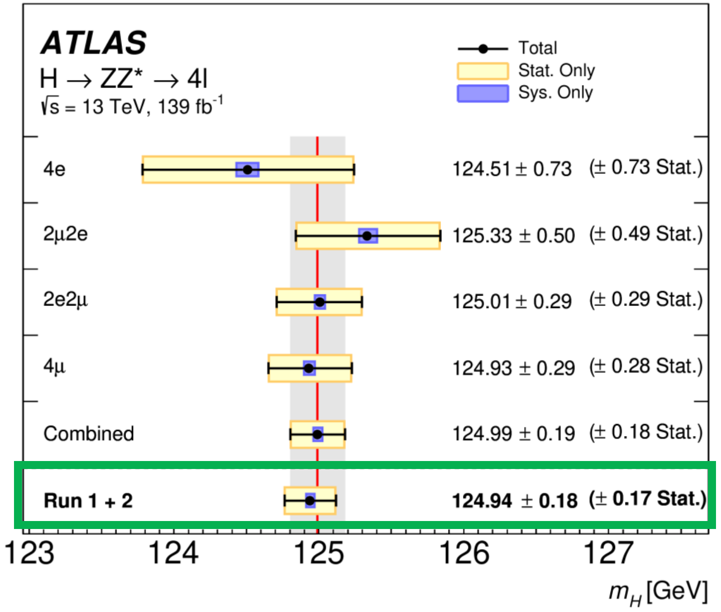

Higgs Boson Mass Measurements

High mass-resolution decay-channels, all Higgs production modes considered (ggF, VBF, VH, ttH, tHq, tHW, bbH)

- $H \rightarrow \gamma\gamma$
  - **High-statistics and sensitivity**
  - **Sensitive to non-resonant background modeling**
- $H \rightarrow ZZ \rightarrow 4l$ ("golden channel")
  - **Lower systematic uncertainty on m_H**
  - **Lower statistics final state but very high purity**

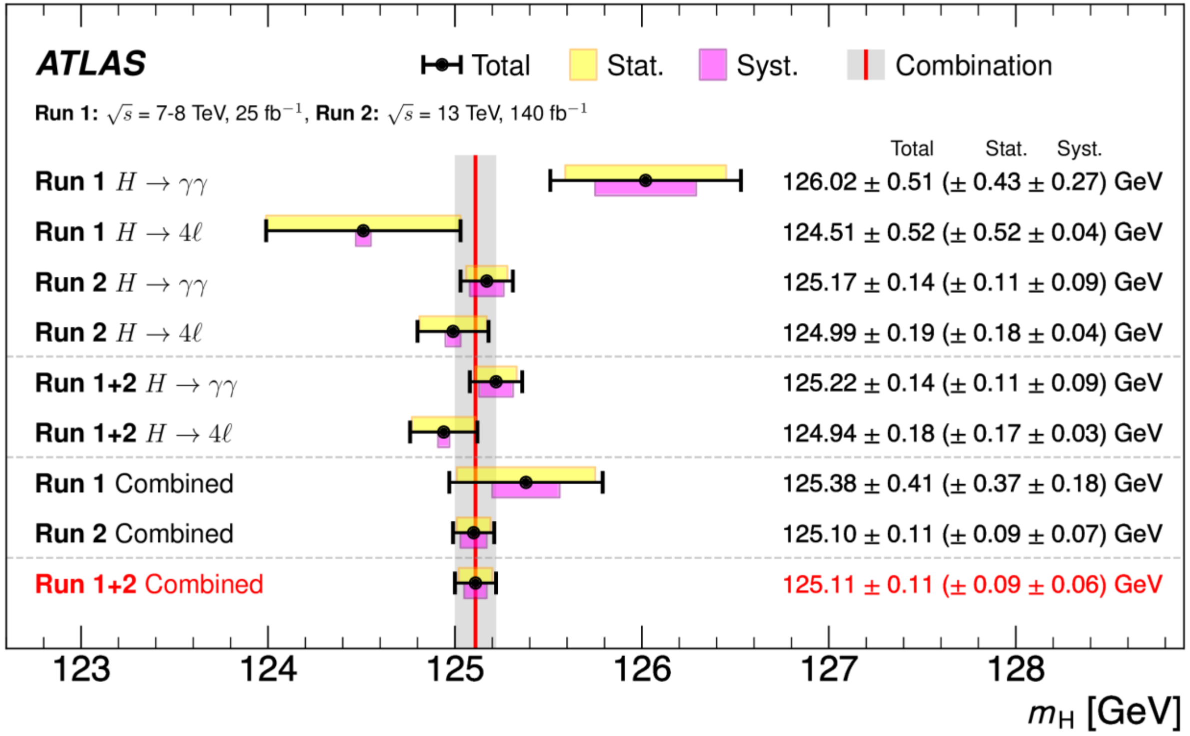

[Phys. Rev. Lett. 131 (2023) 251802]

Combining profile-likelihoods leads to high-precision measurement: $\boxed{\mathbf{m_H = 125.11 \pm 0.11\ GeV}}$

Higgs Width

The Higgs (as measured from **all production modes**) produces a peak in data with an **experimental resolution** $\sim\mathcal{O}(10^3)$ $\mathbf{MeV}$.

Theoretically $\Gamma_H \sim 4.1$ $\mathbf{MeV}$, **far too small to measure directly from line shape**.

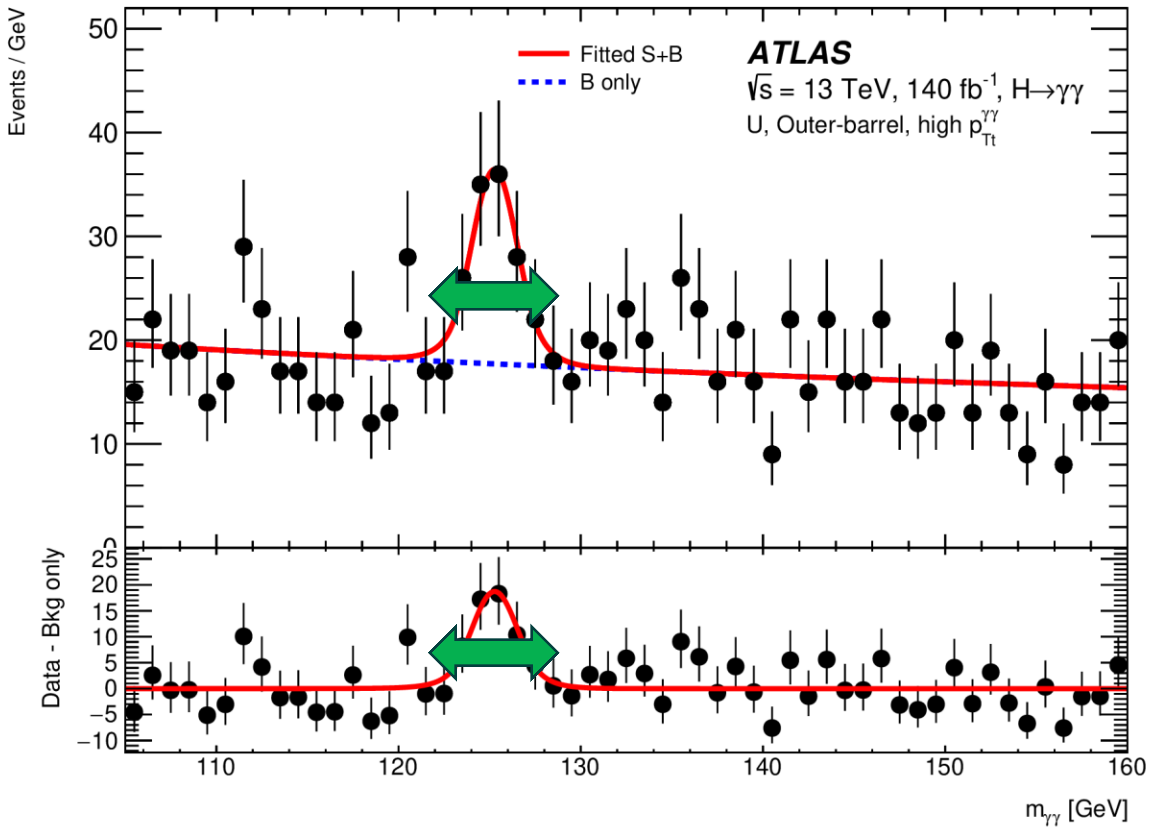

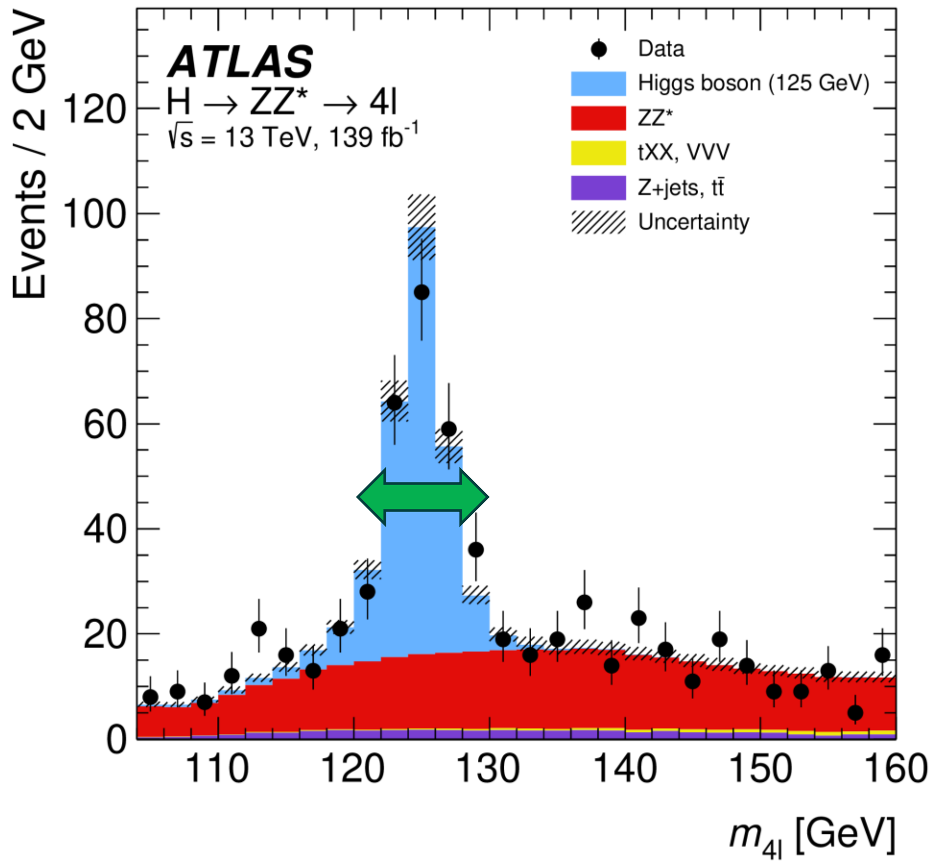

Higgs Width (in V-boson channel)

Breit-Wigner parametrization of the Higgs mass spectrum:

$$\frac{d\sigma_{gg\to H\to ZZ}}{dM_{4l}^2} = \frac{g_{gg\to H}^2 g_{H\to ZZ}^2}{\left(M_{4l}^2 - m_H^2\right)^2 + m_H^2\Gamma_H^2}$$

Under the narrow width approximation: $\sigma_{gg\to H\to ZZ}^{on-shell} \approx \frac{g_{gg\to H}^2 g_{H\to ZZ}^2}{m_H^2\Gamma_H^2}$

In the offshell regime, it's been shown that: $\sigma_{gg\to H\to ZZ}^{off-shell} \approx \frac{g_{gg\to H}^2 g_{H\to ZZ}^2}{M_{4l}^2}$

If the on-shell Higgs couplings **=** off-shell Higgs couplings,

(model dependence)

then $\boxed{\frac{\mu_{off-shell}}{\mu_{on-shell}} \propto \Gamma_H}$ and the **Higgs width is indirectly accessible.**

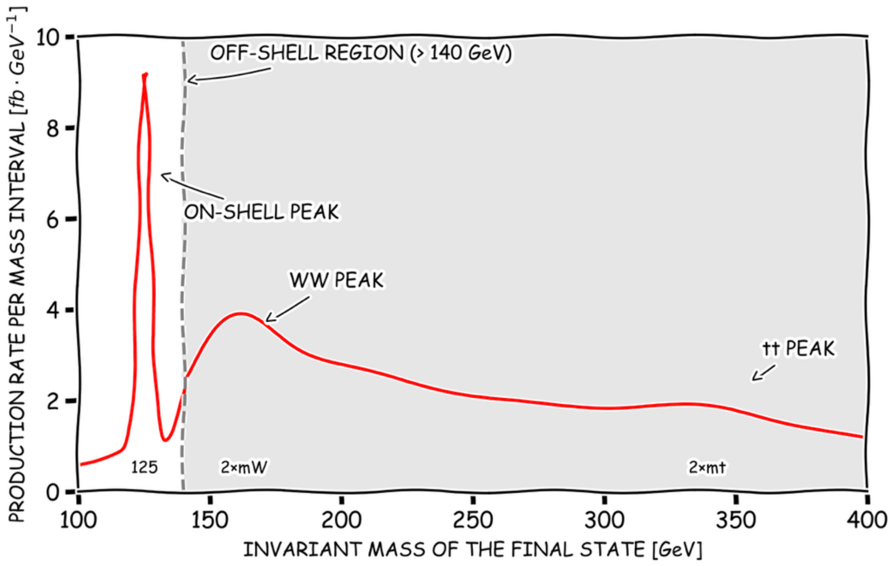

Credit: Zef Wolffs

Previous full Run-2 analysis: Phys. Lett. B 846 (2023) 138223

Width: $H \rightarrow ZZ^* \rightarrow 4l$

Large *destructive* interference in the off-shell regime – nonlinear signal model $p(\vec{x}|\mu) \sim \mu P_S(\vec{x}) + P_B(\vec{x}) + \sqrt{\mu}\, P_I(\vec{x})$

Binned likelihood fit sub-optimal to measure all possible values of $\mu_{off-shell}$

Neural simulation-based inference (NSBI) provides a better estimate of the likelihood ratio (high-dim. probability density ratio) w.r.t a reference distribution $p_{ref}(\vec{x})$

$$-2\ln\mathcal{L}(\mu,\theta,\alpha) = -2\sum_{r}^{regions}\ln[Pois(N_r|\nu_r)] - 2\sum_{i}^{events}\ln\left[\frac{p(\vec{x}|\mu,\theta,\alpha)}{p_{ref}(\vec{x})}\right] + \sum_{m}^{systematics}(\delta\alpha_m)^2$$

See J.Sandesara's talk from yesterday for more on NSBI

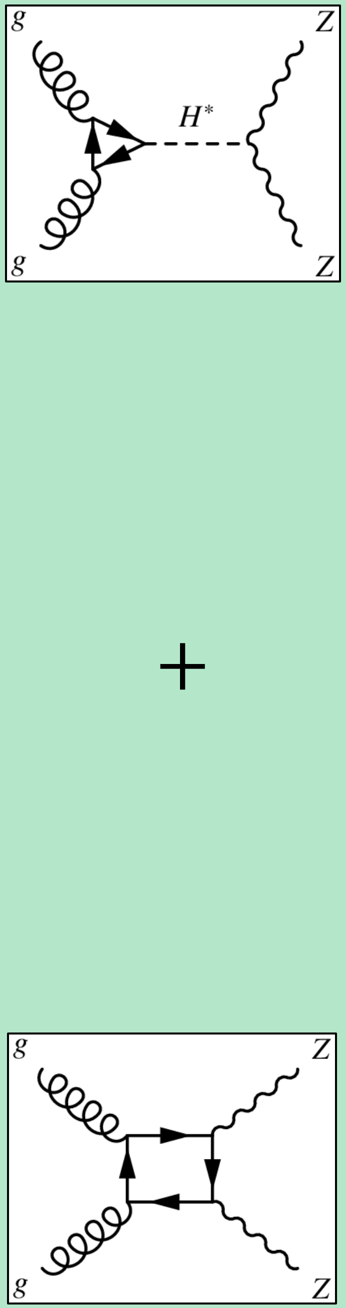

ggF interference

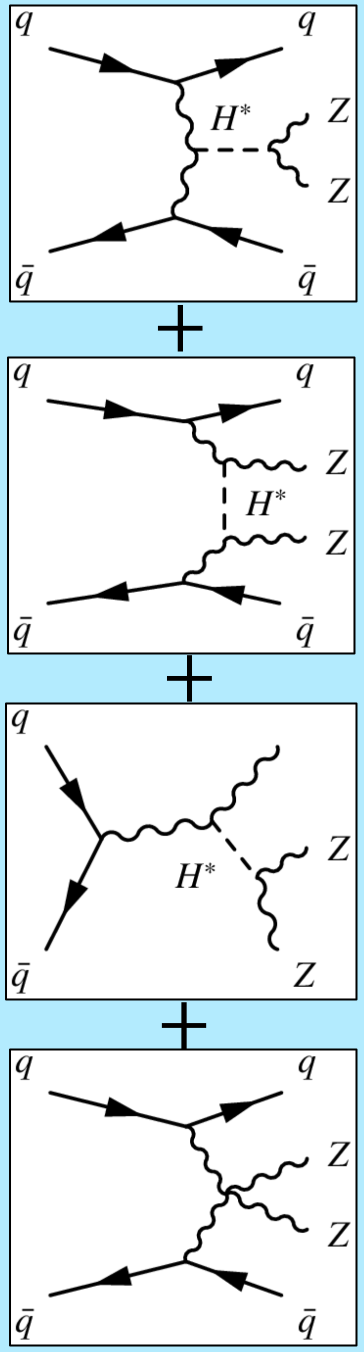

VBF interference

Previous full Run-2 analysis: Phys. Lett. B 846 (2023) 138223

Width: $H \to ZZ^* \to 4l$

LLR (t_μ) is not χ^2 distributed – confidence intervals defined by pseudo-experiments in the Neyman construction

Combination with $H \to ZZ^* \to 2l2\nu$ an observed (expected) sensitivity of 3.7σ (2.4σ) is reached.

$$\mu_{off-shell} = 1.06\,^{+0.62}_{-0.45}\left(1.00\,^{+0.83}_{-0.83}\right)$$

$$\Longrightarrow \boxed{\Gamma_H = 4.3^{+2.7}_{-1.9}\ \left(4.1^{+3.5}_{-3.4}\right)\ \text{MeV}}$$

Moving to a NSBI re-analysis yields a 20% better precision w.r.t histogram-based analysis.

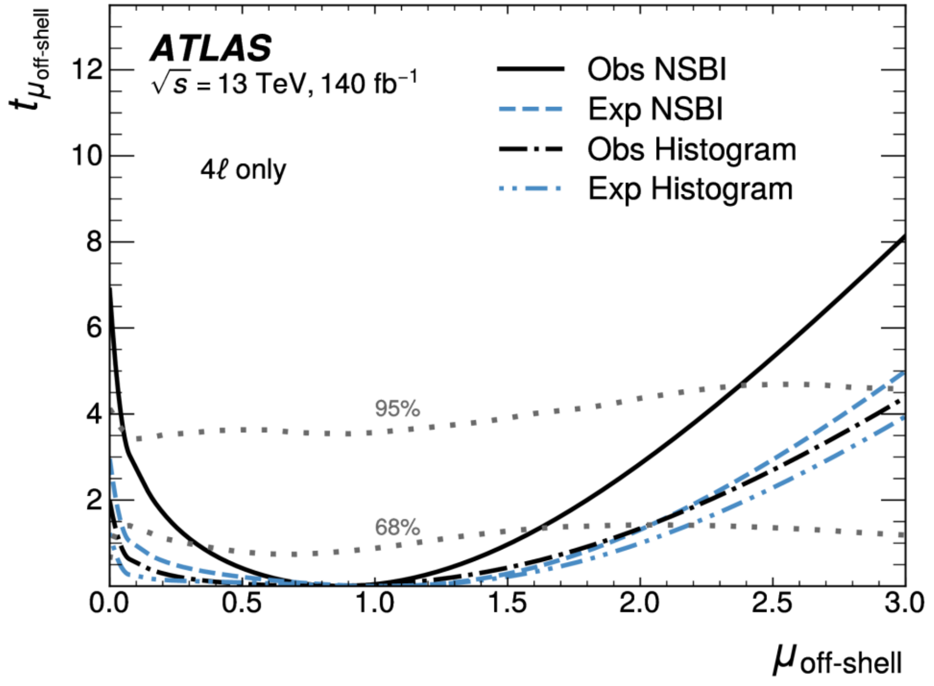

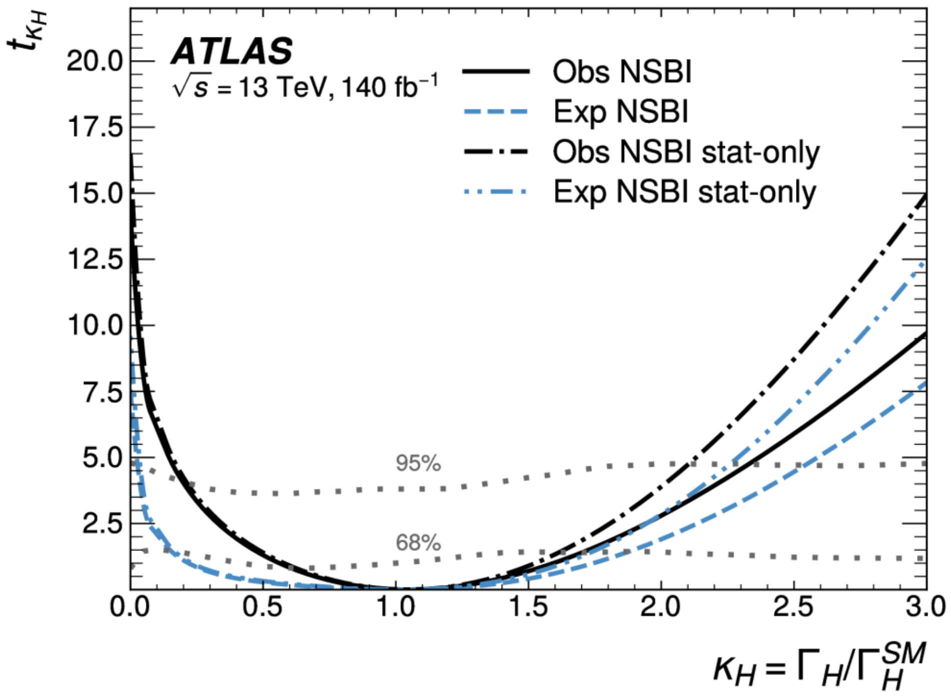

Width: $H \to WW^*$

$H \to WW^* \to 2l2\nu$ is analysed in SF/DF channels and 0, 1, and 2 jet categories (ggF and VBF).

Less ggWW background interference but higher non-interfering (top, qqWW, fakes) background contamination.

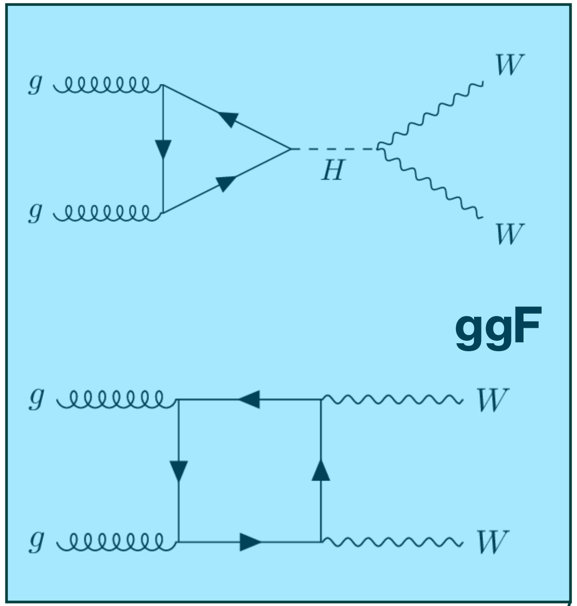

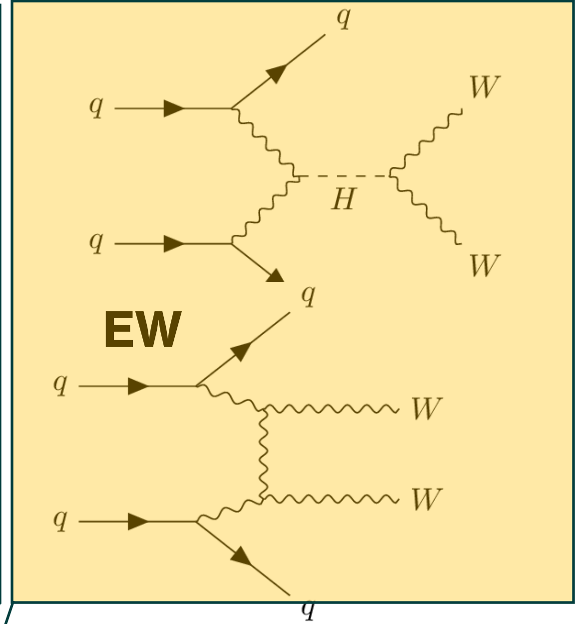

A DNN is trained to separate signal and non-interfering background to define signal- and control-regions

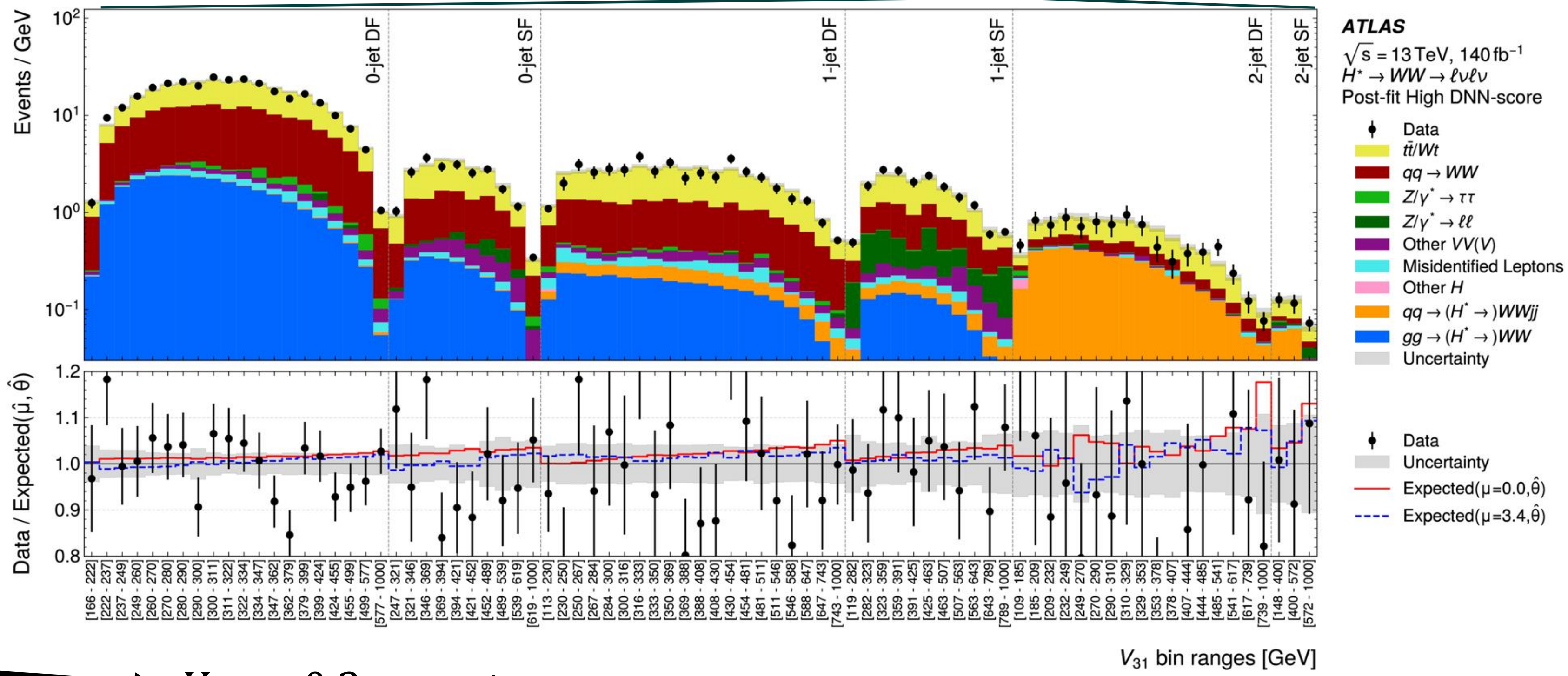

Events in SR are binned in terms of an m_{WW} proxy variable V_{31}.

$$V_{31} = 0.3 * m_{ll} + m_T$$

Previous Run-1 analysis: Eur. Phys. J. C 75 (2015) 335

Width: $H \rightarrow WW^*$

Off-shell $H \rightarrow WW^*$ is constrained to

$\mu_{off-shell} < 3.4\ (4.4)$ at 95% confidence.

$$\boxed{\boldsymbol{\mu_{off-shell} = 0.3^{+0.9}_{-0.3}\left(1.0^{+2.3}_{-1.0}\right)}}$$

$\Longrightarrow \Gamma_H < 13.1\ (17.3)\ MeV$ at 95% confidence

$$\boxed{\boldsymbol{\Gamma_H = 0.9^{+3.4}_{-0.9}\left(4.1^{+8.3}_{-3.8}\right)\ \mathrm{MeV}}}$$

First width interpretation in $H \rightarrow WW^*$ using full Run-2 dataset.

Roughly ~500% improvement over Run-1 measurement!

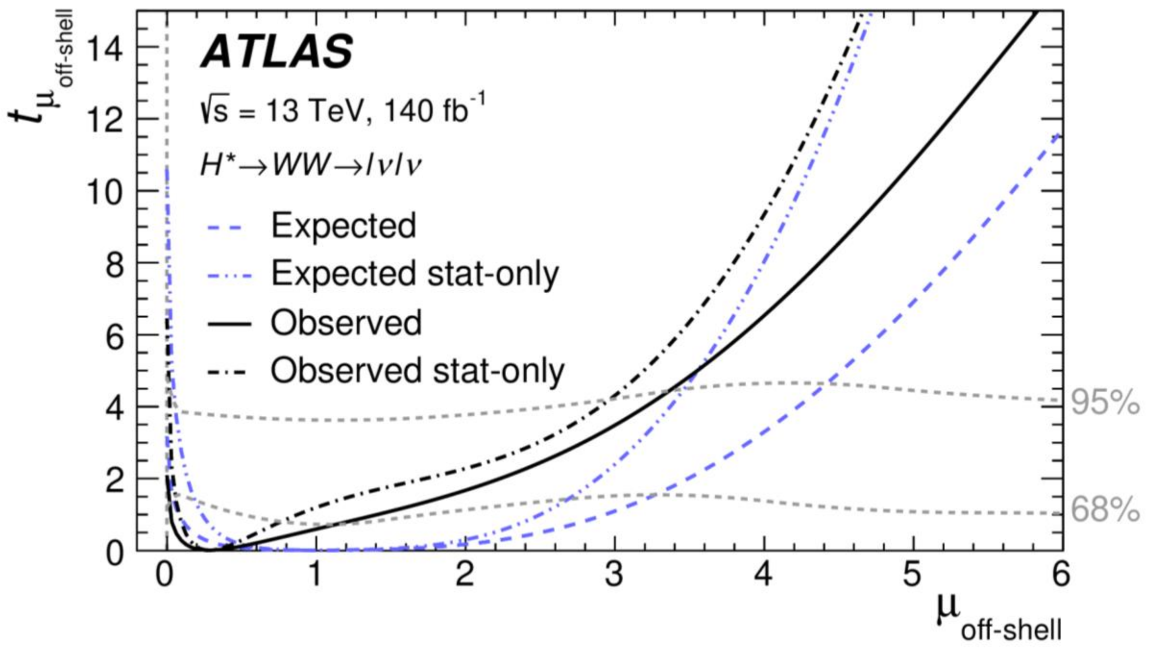

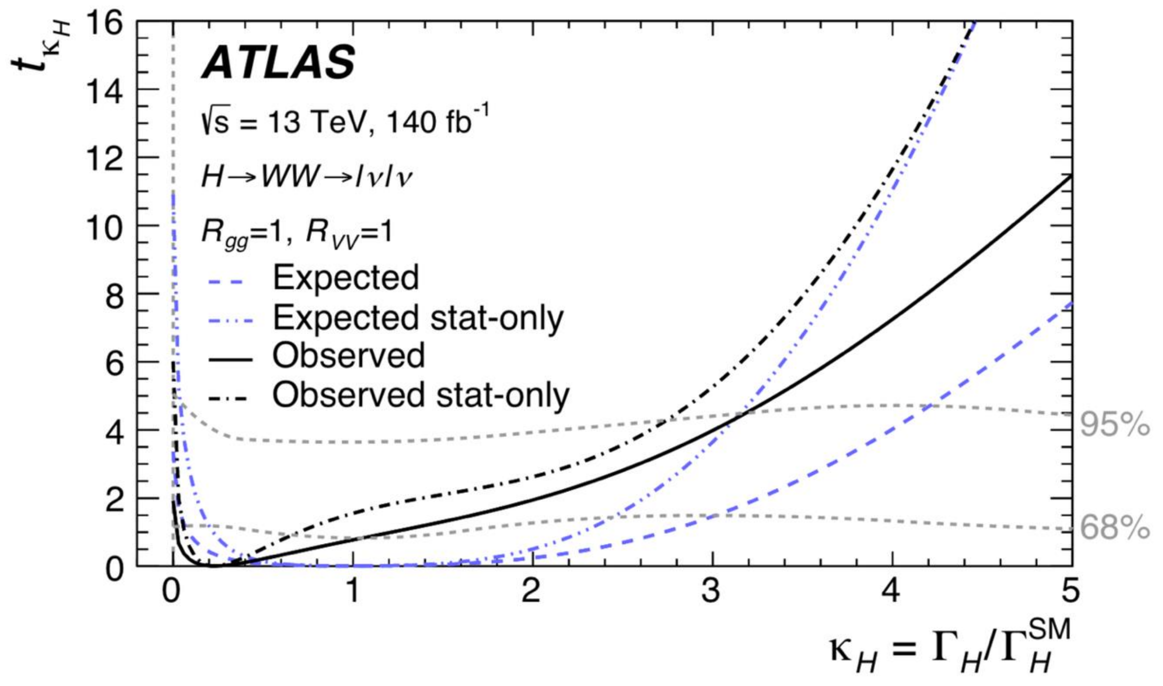

Width: $tt\bar{t}\bar{t}$ + $t\bar{t}H$

The recent 4-top analysis has **significant contributions of off-shell ttH diagrams**

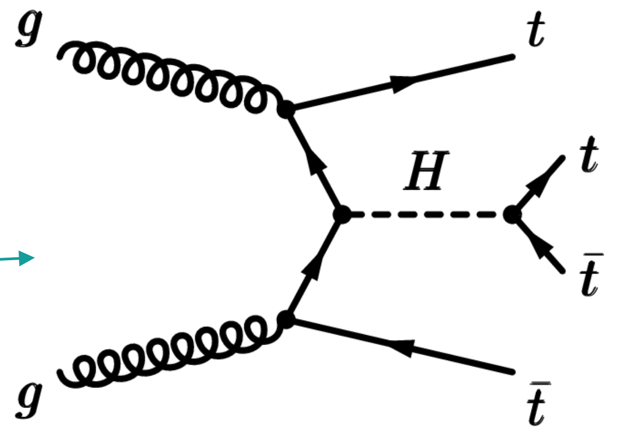

When combined with the recent on-shell ttH measurements, **an interpretation of Γ_H is possible without the same model assumptions as in $H \to VV$**

Best-fit value: $\boldsymbol{\Gamma_H = 86^{+110}_{-49}}$ **MeV** (2σ away from SM)

Upper limit: $\boldsymbol{\Gamma_H < 160\ (55)}$ **MeV** at 95% confidence

This result is the first interpretation of Γ_H in Higgs-Top processes **distinct from $H \to VV$ final states**

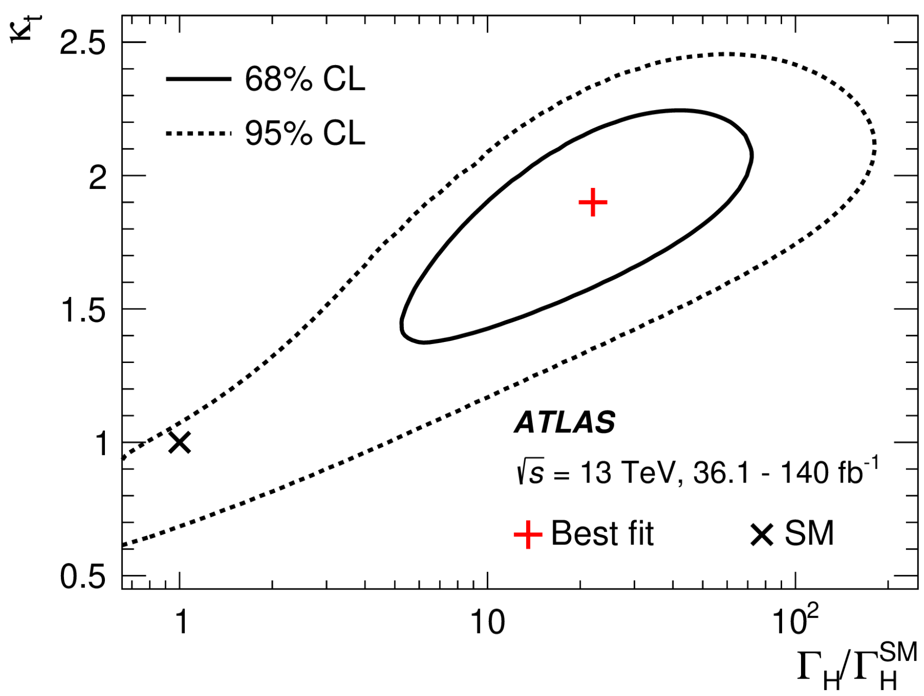

Phys. Lett. B 861 (2025) 139277

Conclusions

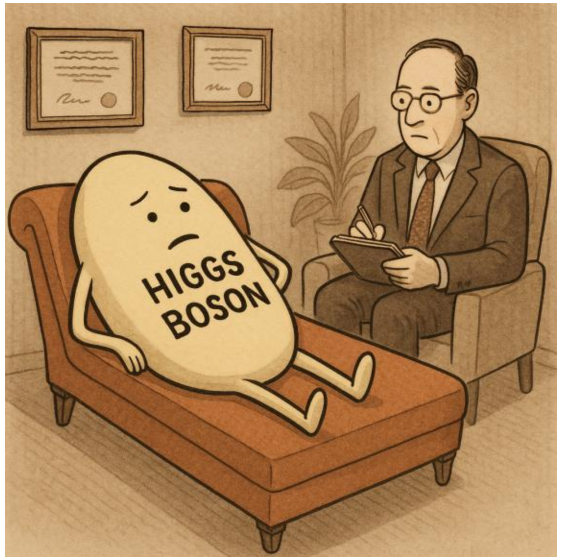

Soon, we can start asking "*How is* the Higgs?"
Image generated by ChatGPT 4o

How *heavy* is the Higgs?

Higgs mass measured to **per-mille level of precision**

- $H \rightarrow \gamma\gamma$ provides the highest precision measurement in a single channel
- $H \rightarrow ZZ$ channel is statistically limited, **improved with Run3/HL-LHC data!**

How *wide* is the Higgs?

Homing in on Higgs width with **indirect measurements**

- **Re-analysis of $H \rightarrow ZZ^*$ with NSBI provides 20% improved precision**
- **First interpretation of Γ_H in $H \rightarrow WW^*$, approaching the precision of $H \rightarrow ZZ^*$**
- Γ_H probed in $t\bar{t}t\bar{t}$ for the first time, with **more to come in Run-3 and HL-LHC!**

Thank you for your attention!

Backup

Mass: $H \to \gamma\gamma$

Events split into 14 categories with higher/lower:

- **Energy scale uncertainties**
- **$m_{\gamma\gamma}$ resolution**
- **Signal–to–background ratio**

$$\langle m\rangle \pm \frac{\sigma_{error}}{\sqrt{N_{signal}}}$$

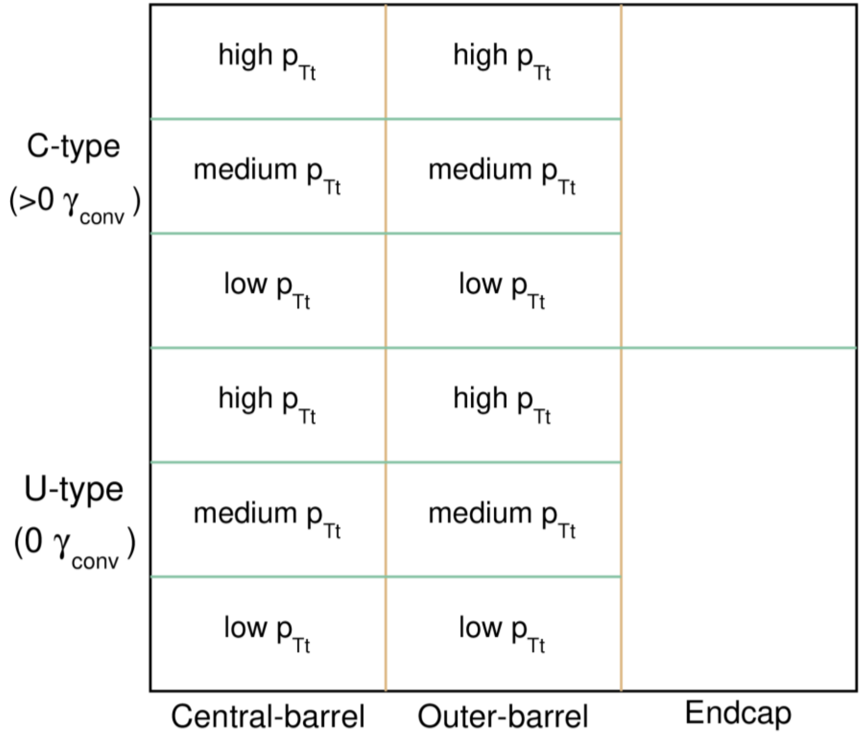

Category splitting based on the di-photon system

Low pT: $p_{Tt}^{\gamma\gamma}$ < 70 GeV

Medium pT: 70 < $p_{Tt}^{\gamma\gamma}$ < 130 GeV

High pT: $p_{Tt}^{\gamma\gamma}$ > 130 GeV

Central: $|\eta| < 0.8$

Outer-barrel: $|\eta| < 1.37$, at least one with $|\eta| > 0.8$

End-cap: at least one with $1.52 \leq |\eta| < 2.37$

$p_{Tt}^{\gamma\gamma} = |\vec{p}_T^{\gamma\gamma} \times \hat{t}|$ **where** $\hat{t} = \frac{\vec{p}_T^{\gamma 1} - \vec{p}_T^{\gamma 2}}{|\vec{p}_T^{\gamma 1} - \vec{p}_T^{\gamma 2}|}$

Width w/ 90% of signal

Category	$\sigma_{90}^{\gamma\gamma}$ [GeV]	S_{90}	B_{90}	f_{90} [%]	Z_{90}
U, Central-barrel, high $p_{Tt}^{\gamma\gamma}$	1.88	42	65	39.1	4.7
U, Central-barrel, medium $p_{Tt}^{\gamma\gamma}$	2.34	102	559	15.4	4.2
U, Central-barrel, low $p_{Tt}^{\gamma\gamma}$	2.63	837	13 226	6.0	7.2
U, Outer-barrel, high $p_{Tt}^{\gamma\gamma}$	2.16	31	83	27.4	3.3
U, Outer-barrel, medium $p_{Tt}^{\gamma\gamma}$	2.63	108	981	9.9	3.4
U, Outer-barrel, low $p_{Tt}^{\gamma\gamma}$	3.00	869	22 919	3.7	5.7
U, Endcap	3.33	759	29 383	2.5	4.4
C, Central-barrel, high $p_{Tt}^{\gamma\gamma}$	2.10	26	44	37.3	3.6
C, Central-barrel, medium $p_{Tt}^{\gamma\gamma}$	2.62	62	389	13.8	3.1
C, Central-barrel, low $p_{Tt}^{\gamma\gamma}$	3.00	508	9 726	5.0	5.1
C, Outer-barrel, high $p_{Tt}^{\gamma\gamma}$	2.56	34	103	25.0	3.2
C, Outer-barrel, medium $p_{Tt}^{\gamma\gamma}$	3.20	114	1 353	7.8	3.1
C, Outer-barrel, low $p_{Tt}^{\gamma\gamma}$	3.71	914	30 121	2.9	5.2
C, Endcap	4.04	1 249	52 160	2.3	5.5
Inclusive	3.32	5 653	128 774	4.2	15.6

Mass: $H \to \gamma\gamma$

Significant improvements from **new photon reconstruction algorithm** and **photon energy calibration** using large $Z \to e^+e^-$ data set

Photon energy calibration : 320 MeV → 83 MeV

- $Z \to e^+e^-$ electron energy **linearity fit**
- Constrain electron E_T-dependent energy scale

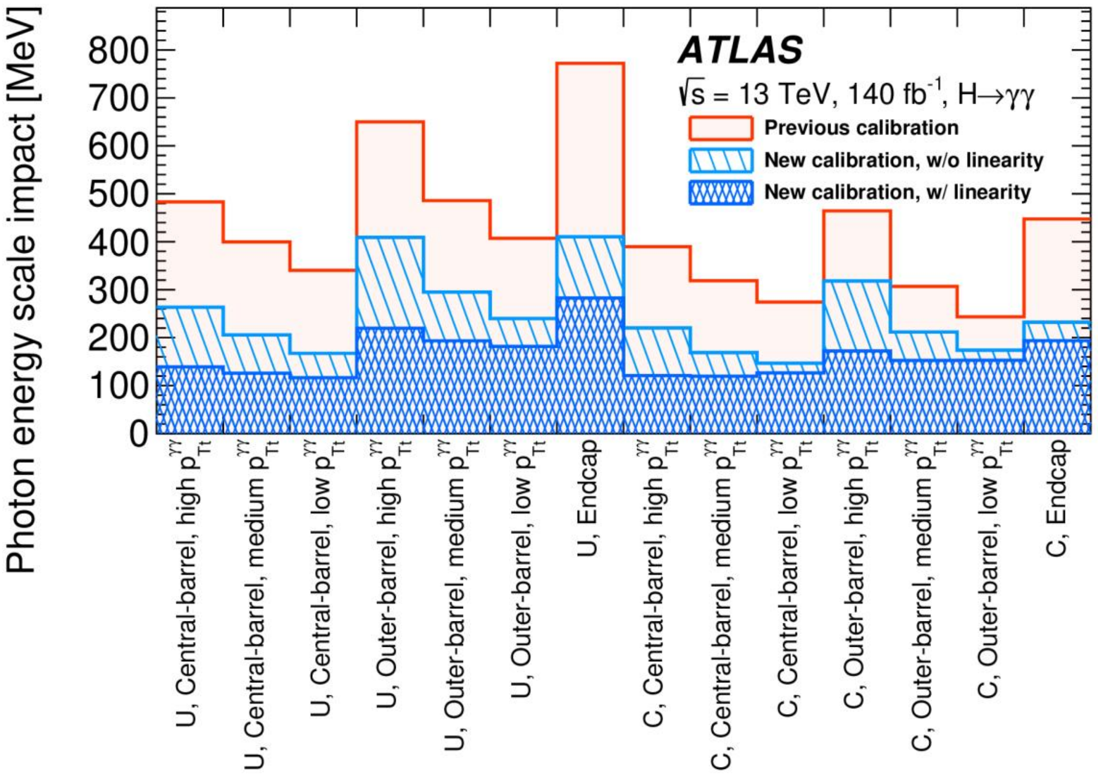

Reduction in photon energy scale uncertainty from with E_T-dependent linearity fit across all analysis regions

Mass: $H \rightarrow ZZ \rightarrow 4l$

Non-resonant ZZ backgrounds separated from signal by a **classification DNN**, trained with p_T^{4l}, η^{4l}, and a **matrix-element discriminant:** $D_{ZZ} = \ln\left(\frac{|\mathcal{M}_{sig}|^2}{|\mathcal{M}_{bkg}|^2}\right)$

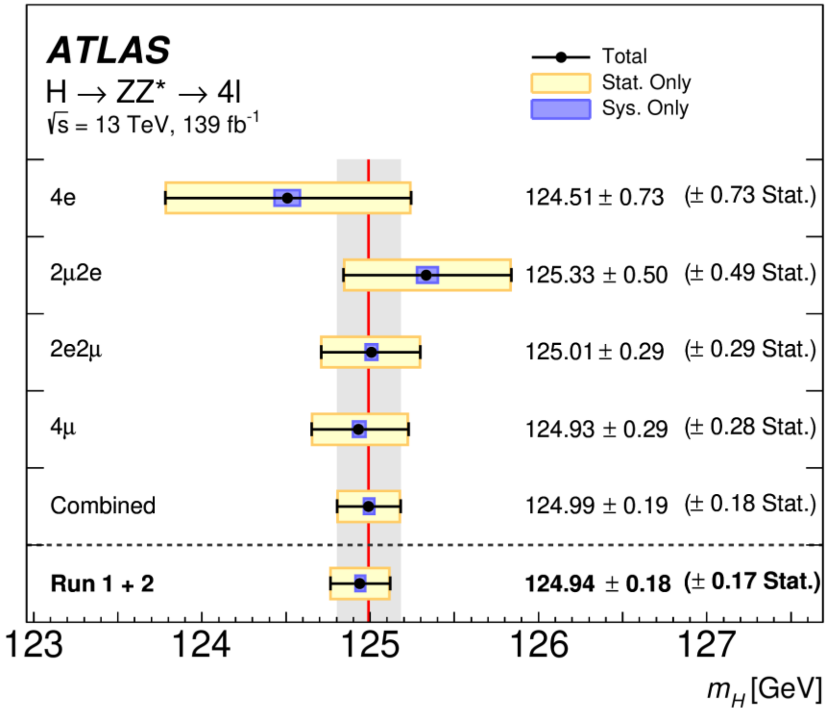

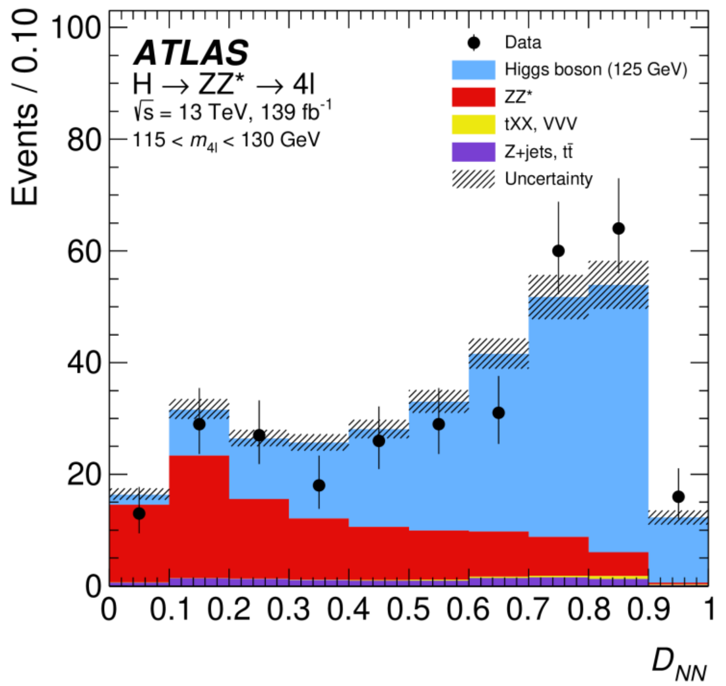

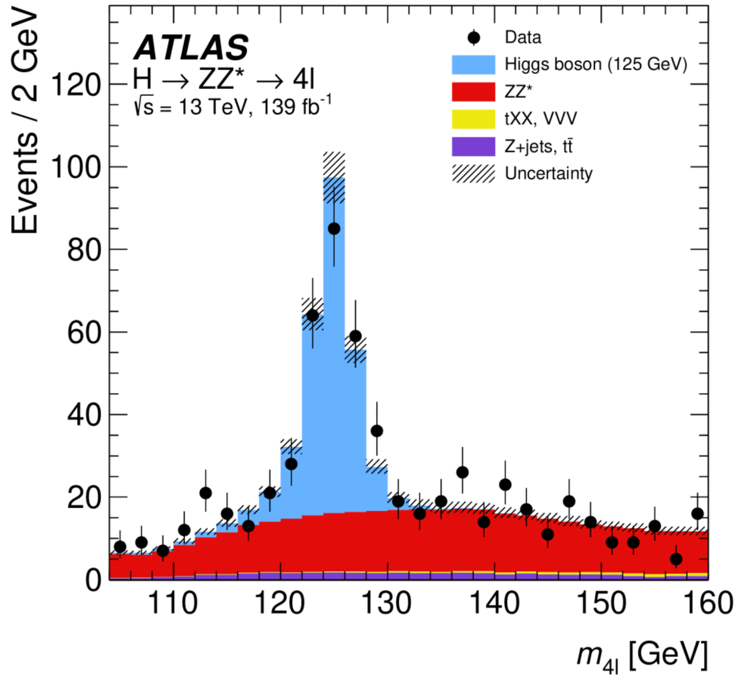

Width: $H \rightarrow ZZ^*$

Neural simulation-based inference (NSBI) model is trained in SR

Variable	Definition
$m_{4\ell}$	quadruplet mass
m_{Z_1}	Z_1 mass
m_{Z_2}	Z_2 mass
$\cos\theta^*$	cosine of the Higgs boson decay angle $[\mathbf{q}_1 \cdot \mathbf{n}_z/\lvert\mathbf{q}_1\rvert]$
$\cos\theta_1$	cosine of the Z_1 decay angle $[-(\mathbf{q}_2)\cdot\mathbf{q}_{11}/(\lvert\mathbf{q}_2\rvert\cdot\lvert\mathbf{q}_{11}\rvert)]$
$\cos\theta_2$	cosine of the Z_2 decay angle $[-(\mathbf{q}_1)\cdot\mathbf{q}_{21}/(\lvert\mathbf{q}_1\rvert\cdot\lvert\mathbf{q}_{21}\rvert)]$
Φ_1	Z_1 decay plane angle $[\cos^{-1}(\mathbf{n}_1\cdot\mathbf{n}_{\mathrm{sc}})\,(\mathbf{q}_1\cdot(\mathbf{n}_1\times\mathbf{n}_{\mathrm{sc}})/(\lvert\mathbf{q}_1\rvert\cdot\lvert\mathbf{n}_1\times\mathbf{n}_{\mathrm{sc}}\rvert)]$
Φ	angle between Z_1, Z_2 decay planes $[\cos^{-1}(\mathbf{n}_1\cdot\mathbf{n}_2)\,(\mathbf{q}_1\cdot(\mathbf{n}_1\times\mathbf{n}_2)/(\lvert\mathbf{q}_1\rvert\cdot\lvert\mathbf{n}_1\times\mathbf{n}_2\rvert)]$
$p_T^{4\ell}$	quadruplet transverse momentum
$y^{4\ell}$	quadruplet rapidity
n_{jets}	number of jets in the event
m_{jj}	leading dijet system mass
$\Delta\eta_{jj}$	leading dijet system pseudorapidity
$\Delta\phi_{jj}$	leading dijet system azimuthal angle difference

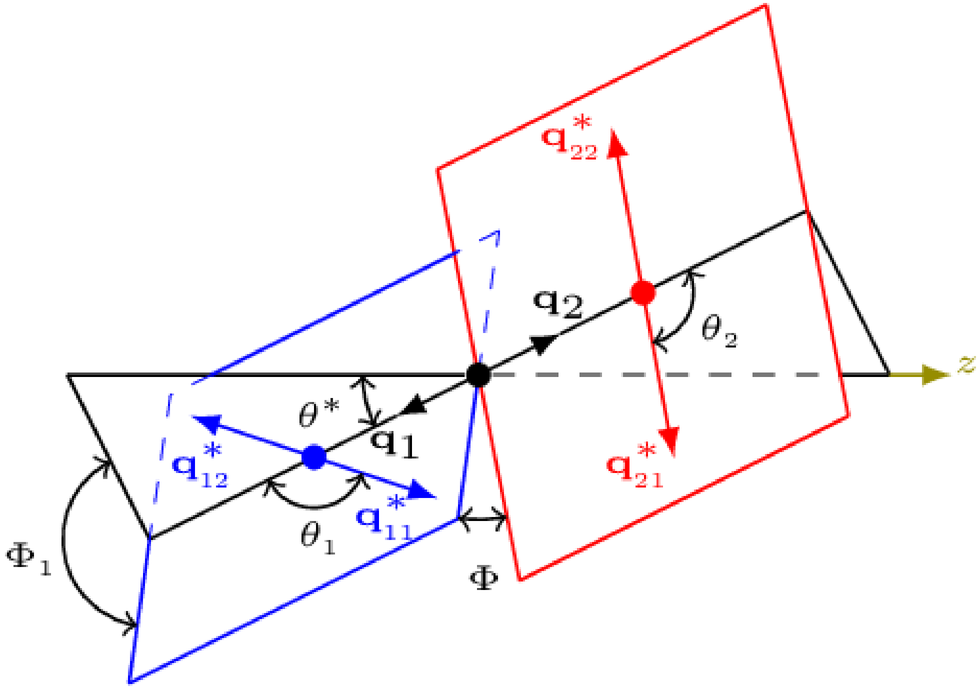

Ensembles of fully connected NNs are trained w/ 10-fold cross-validation (80:20 training split per fold)
~10-70 ensembles are trained to **estimate probability density ratios** w.r.t. a reference PDF.
$p_{ref}(x) \sim p_S(x)$ **(signal model) is chosen to ensure numerical stability of the model in the SR.**

Width: $H \rightarrow ZZ^*$

The NSBI method directly estimates the probability density ratio on a per-event basis.

Comparing the NSBI prediction directly with a binned likelihood estimate of the same, a **calibration curve** can show it is an unbiased estimator.

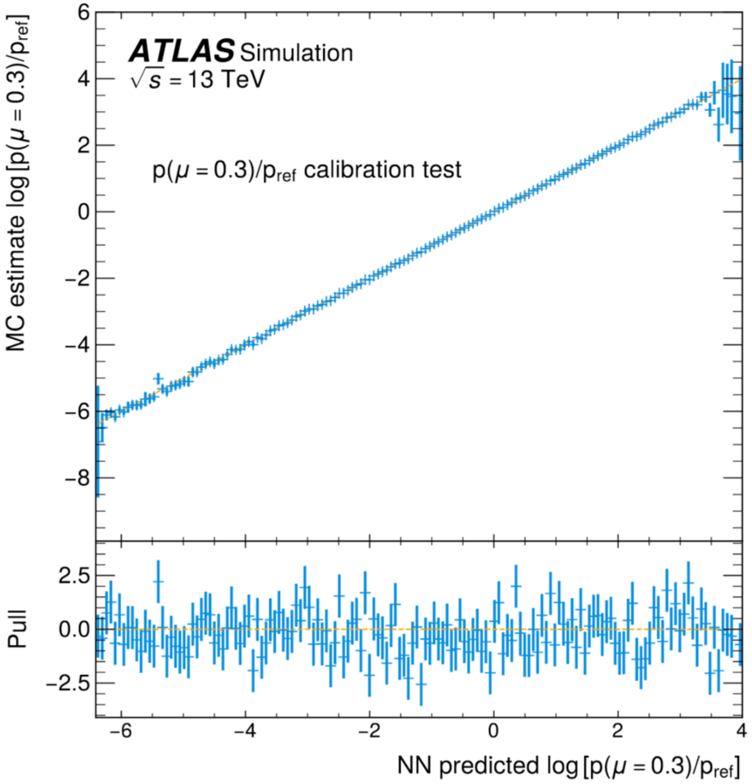

Interference dominated off-shell signal model

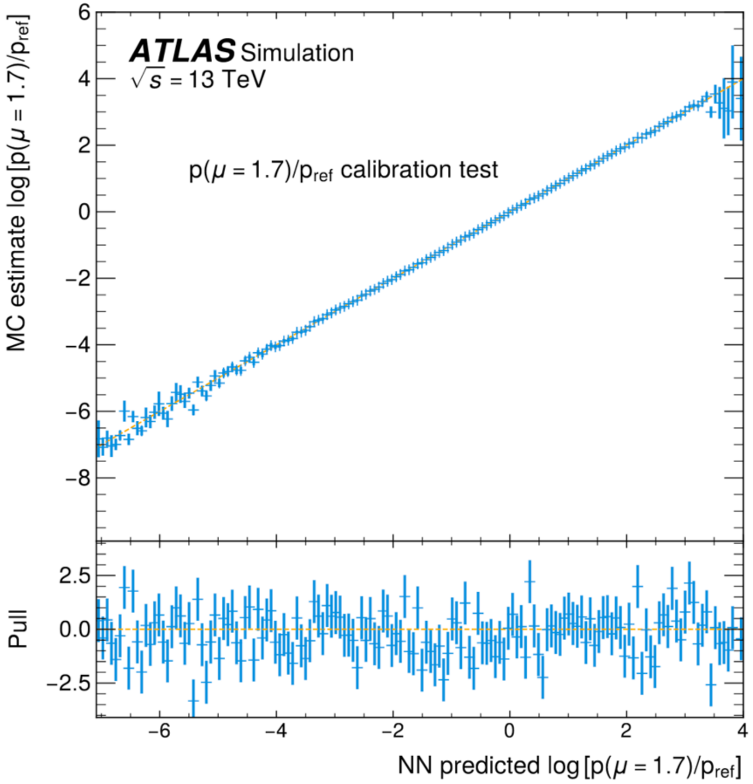

Signal dominated off-shell signal model

Width: $H \to ZZ^*$

The interference in the signal region generates **double-minima** in the likelihood function.

This degeneracy can be lifted within the NSBI prescription, as a multi-dimensional phase-space is used in estimating the probability density ratio.

In $H \to ZZ^*$, toy models are used to generate the precise confidence intervals using the Neyman construction.

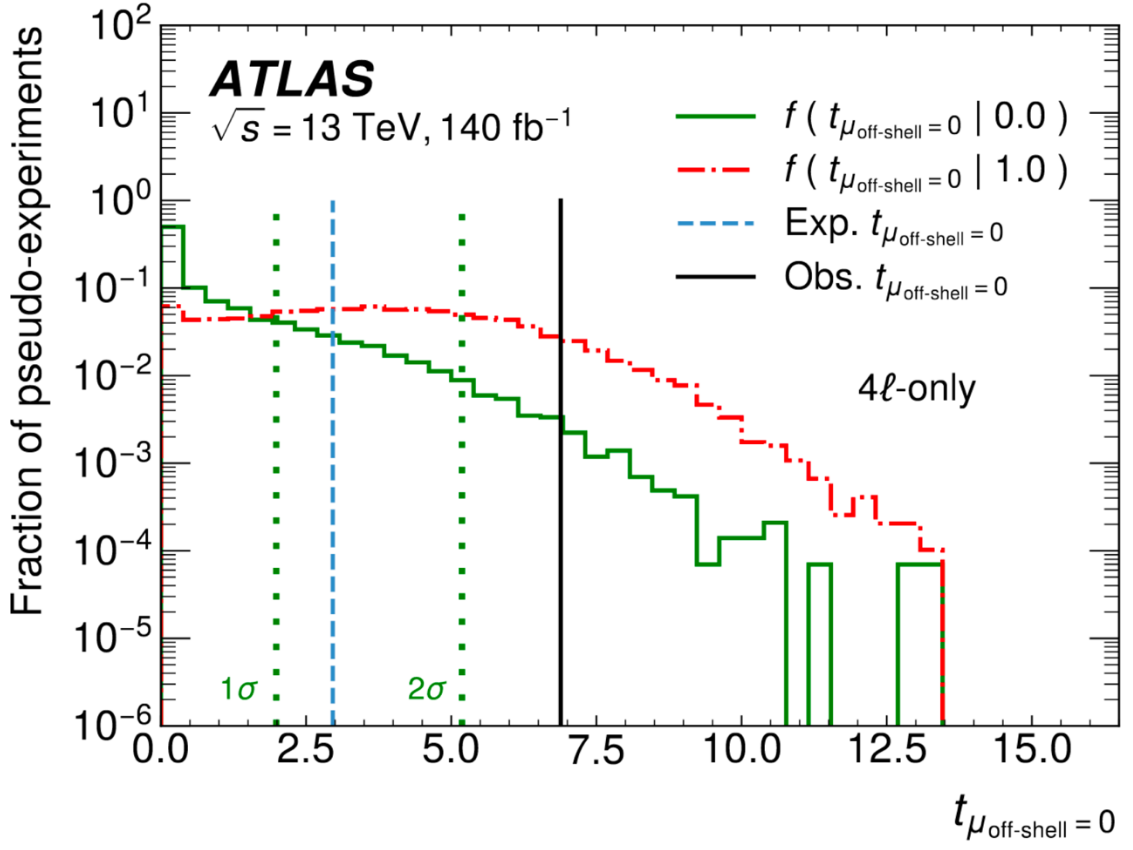

Width: $H \rightarrow WW^*$

The V_{31} mass-proxy variable relates the lepton pair transverse-momenta, invariant mass, and transverse mass

$$V_{xy} = x\, m_{ll} + y\, m_T$$

where $m_T = \sqrt{\left(E_T^{ll} - E_T^{miss}\right)^2 - \left|p_T^{ll} - E_T^{miss}\right|^2}$

and $E_T^{ll} = \sqrt{\left|p_T^{ll}\right|^2 - m_{ll}^2}$

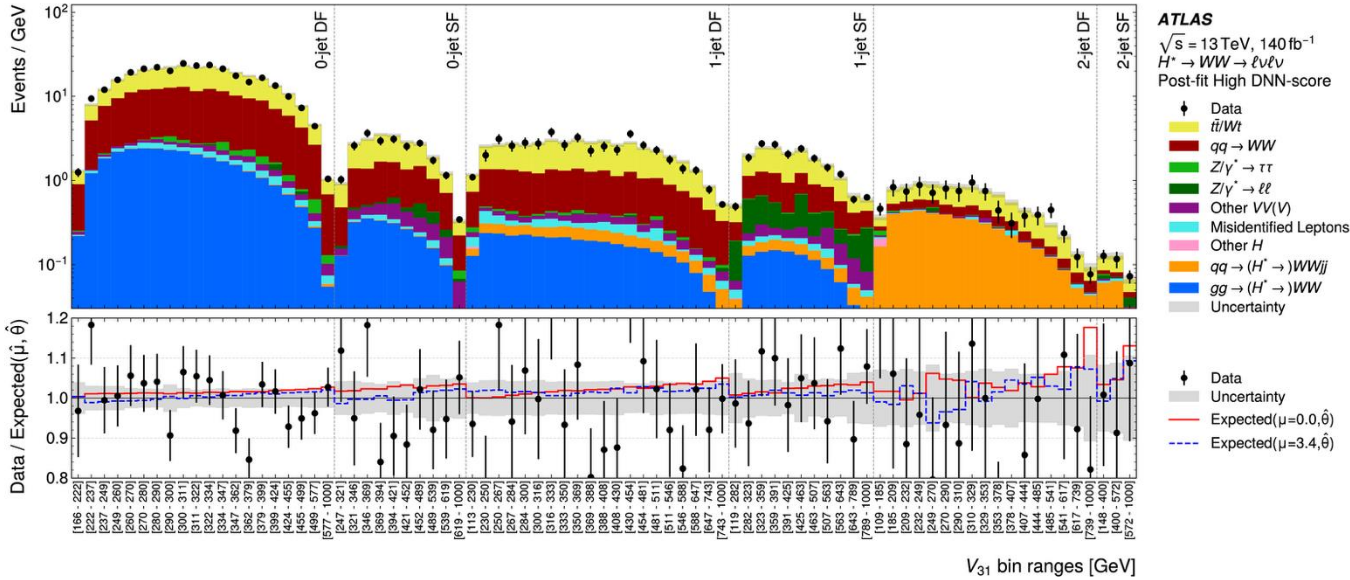

The V_{31} variable has x=0.3, y=1.0, tuned to give the best proxy of the true m_{WW} (smallest bias with highest correlation to m_{WW})